CHAPTER VI

FLUX CREEP-FLOW MODEL

Edmund Soji Otabe and Masaru Kiuchi

Faculty of Computer Science and Systems Engineering,
Kyushu Institute of Technology,
680–4 Kawazu, Iizuka 820–8502, Japan
otabe@cse.kyutech.ac.jp

I. INTRODUCTION

Since oxide superconductor is used at high temperatures and flux pinning is weak, thermal agitation of flux lines is significant resulting in high relaxation of shielding current compared with conventional metal superconductor. For example, when magnetic field is trapped by bulk oxide superconductor, the trapped magnetic field decreases according to time. This effect is known as flux creep and firstly explained by Anderson and Kim[1]. That is, the trapped flux line by pinning center is thermally agitated and it could move to the direction of Lorentz force. This causes reduction of the trapped magnetic field and the shielding current. When current density in superconductor is sufficiently small, flux lines move time to time (flux creep) and very small electric field is induced. Therefore it is not continuous flow but discontinuous hopping. On the contrary, when the current density becomes high, continuous movement of the flux lines (flux flow) is dominant.

Electromagnetic properties such as, characteristics of electric field and current density (E-J), critical current density (J_c), irreversibility field (B_i) in oxide superconductor are well explained by flux creep-flow model. In this chapter, the flux creep phenomenon is firstly explained and then, numerical and analytical calculations based on flux creep-flow model is described. Finally, some experimental results are compared with prediction by the flux creep-flow model.

II. FLUX CREEP PHENOMENON

II.1. *Flux creep*

When magnetic field is applied to a superconductor, magnetic field penetrates to the superconductor and flux lines are pinned by pinning center. At the same time, flux line tends to move by Lorentz force. These condition is schematically shown in Fig. 1. The energy is periodically changed and decreasing according to increasing the position, x. The gradual decrease is representing the work done by the Lorentz force. In this figure, flux lines move in group unit and this group is called a flux bundle.

According to flux creep model, the possibility to jump over an energy barrier (activation energy), U, for one trial of flux bundle is given by $\exp(-U/K_BT)$ which is known as Arrhenius expression. Here, k_B is Boltzmann constant and k_BT is thermal

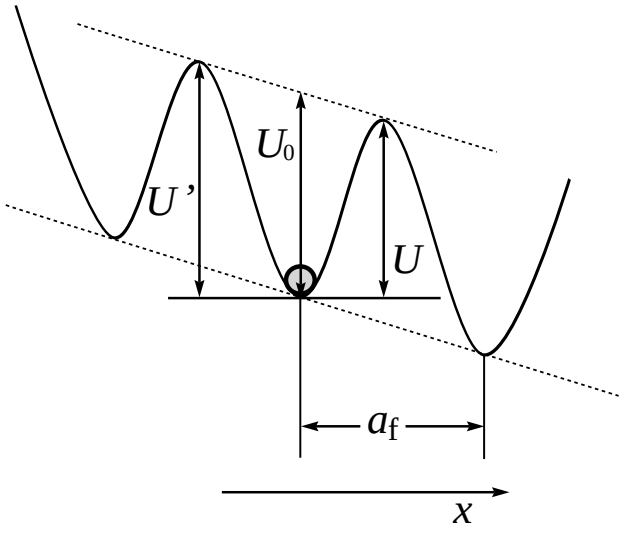

Fig. 1. washboard pinning potential.

energy. If flux bundle succeeded to jump over the activation energy, hopping distance is considered to be given by flux line spacing, a_{f}. According to the movement of the flux bundle, electric field is induced as

$$E = Ba_{\mathrm{f}}\nu_0 \left[\exp\left(-\frac{U}{k_{\mathrm{B}}T}\right) - \exp\left(-\frac{U'}{k_{\mathrm{B}}T}\right)\right], \tag{1}$$

where ν_0 is attempt frequency of the flux bundle, and U' is activation energy of opposite direction to Lorentz force.

Here, we shall calculate a simple case of the relaxation of magnetization by the flux creep. A large slab superconductor ($0 \leq x \leq 2d$) is placed in external magnetic field, H_{e} along z-axis. From the symmetry, we consider only the half region of $0 \leq x \leq d$. In the case of increasing magnetic field, induced current flows along y-axis and movement of the flux bundle by the flux creep is along x-axis. If the current density, J is assumed to be uniform, magnetic flux density is given by $B = \mu_0(H_{\mathrm{e}} - Jx)$. Therefore, observed electric field, E, at the surface of superconductor ($x = 0$) is calculated from Maxwell equation, $\mathrm{rot}\boldsymbol{E} = -\partial\boldsymbol{B}/\partial t$ and is given by

$$E = \frac{\partial d\langle B\rangle}{\partial t} = -\frac{\mu_0 d^2}{2}\cdot\frac{\partial J}{\partial t}, \tag{2}$$

where $\langle B\rangle$ is the average of magnetic flux density. If we have the relations, $U(J)$ and $U'(J)$ as function of J, relaxation of J as a function of time is obtained by substituting Eq. (1) to Eq. (2).

When the relaxation is small, the effect of the flux creep is small. Then it is supposed $U \ll U'$ and the second term of Eq. (1) can be neglected. Since U decreases with increasing of J, U can be expanded to

$$U = U_0^* - rJ. \tag{3}$$

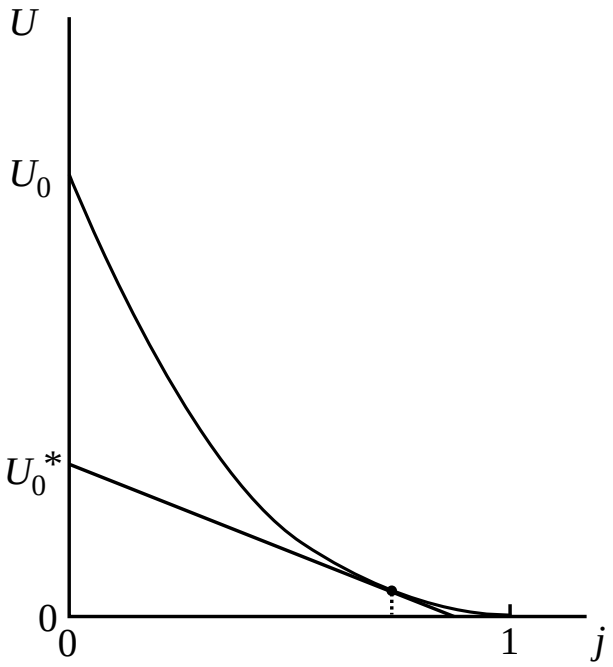

Fig. 2. Relation between activation energy, U, and normalized current density, $j = J/J_{c0}$.

Here U_0^* is the energy at $J \to 0$ and is called the apparent pinning potential as shown in Fig. 2. U_0^*, which is experimentally measured in relaxation rate of magnetization, is different from true pinning potential U_0. Because U_0 is only observed at $J \to 0$ and Eq. (3) is useful at $J \sim J_{c0}$, where J_{c0} is virtual critical current density obtained at $U = 0$. In other words, virtual critical current density is observed at the case of flux creep free. Therefore, it is approximately considered $r = U_0^*/J_{c0}$, and U is given by

$$U = U_0^* \left(1 - \frac{J}{J_{c0}}\right). \tag{4}$$

Hence Eqs. (1), (2) and (4), we have

$$\frac{\partial J}{\partial t} = -\frac{2Ba_f\nu_0}{\mu_0 d^2} \exp\left[-\frac{U_0^*}{k_B T}\left(1 - \frac{J}{J_{c0}}\right)\right]. \tag{5}$$

This equation is easily solved under the condition $J = J_{c0}$ at $t = 0$ and we obtain

$$\frac{J}{J_{c0}} = 1 - \frac{k_B T}{U_0^*} \log\left(\frac{2Ba_f\nu_0 U_0^* t}{\mu_0 d^2 J_{c0} k_B T} + 1\right). \tag{6}$$

Therefore, after a sufficient time, 1 in the argument of logarithm can be neglected. In this case, the logarithmic relaxation rate is given by

$$-\frac{\mathrm{d}}{\mathrm{d}\log t}\left(\frac{J}{J_{c0}}\right) = \frac{k_B T}{U_0^*}, \tag{7}$$

and U_0^* is obtained from experimental result. In usual case of experiment of relaxation of magnetization, initial magnetization, M_0, is used and in this case $J/J_{c0} \to M/M_0$ for Eq. (7).

According to the result investigated by Welch[2], the relation between apparent pinning potential and true pinning potential is given for sinusoidal pinning potential well as

$$U_0^* = 1.65(k_{\rm B}TU_0^2)^{1/3}. \tag{8}$$

Therefore, true pinning potential can be estimated from apparent pinning potential observed from relaxation of magnetization.

II.2. *Flux creep in sinusoidal washboard potential*

Here we estimate current density dependence of activation energy, $U(j)$, for sinusoidal washboard potential as shown in Fig. 2, where j is normalized current density given by $j = J/J_{\rm c0}$. The washboard potential is assumed by

$$F(x) = \frac{U_0}{2}\sin\, kx - fx \tag{9}$$

as shown in Fig. 1. In the above $k = 2\pi/a_{\rm f}$ and $f = JBV$ is Lorentz force to the flux bundle, where V is volume of flux bundle. The local equilibrium position of the flux bundle is obtained by differentiating of Eq. (9) and given by

$$x = -x_0 = -\frac{1}{k}\cos^{-1}\left(\frac{2f}{U_0k}\right). \tag{10}$$

On the other hand, $F(x)$ is maximum at $x = x_0$. Therefore activation energy is obtained by $U = F(x_0) - F(-x_0)$ and is

$$\frac{U}{U_0} = \left[1 - \left(\frac{2f}{U_0k}\right)^2\right]^{1/2} - \left(\frac{2f}{U_0k}\right)\cos^{-1}\left(\frac{2f}{U_0k}\right). \tag{11}$$

If there is no thermal agitation, virtual critical state is achieved and $U = 0$ is obtained. In this case, x_0 is equal to 0 and $2f/U_0k = 1$ is satisfied. Therefore, J is equal to virtual critical current density in the case of flux creep free, $J_{\rm c0}$. Hence, following relation is obtained,

$$\left(\frac{2f}{U_0k}\right) = \frac{J}{J_{\rm c0}} \equiv j. \tag{12}$$

From this equation, Eq. (11) is written as

$$U(j) = U_0[(1-j^2)^{1/2} - j\cos^{-1}j]. \tag{13}$$

From the relationship,

$$U' \simeq U + \pi U_0\frac{J}{J_{\rm c0}}, \tag{14}$$

Eq. (1) can be written by

$$E = Ba_{\rm f}\nu_0\exp\left[-\frac{U(j)}{k_{\rm B}T}\right]\left[1 - \exp\left(-\frac{\pi U_0 j}{k_{\rm B}T}\right)\right]. \tag{15}$$

Therefore, E-J characteristics can be calculated under the assumption of U_0 and $J_{\rm c0}$.

Attempt frequency of the flux bundle, ν_0, for flux creep is investigated[3] and given by

$$\nu_0 = \frac{\zeta \rho_{\rm f} J_{\rm c0}}{2\pi a_{\rm f} B}, \tag{16}$$

where ζ is a constant depended on the kind of pinning center and $\zeta \simeq 2\pi$ is obtained for the case of point like pinning center [4], $\zeta = 4$ is obtained for the case of large normal pinning center [5]. $\rho_{\rm f}$ is flow resistivity and according to Bardeen-Stephen model [6], $\rho_{\rm f}$ is related with $\rho_{\rm n}$ and given by

$$\rho_{\rm f} = \frac{B}{B_{\rm c2}} \rho_{\rm n}. \tag{17}$$

$\rho_{\rm n}$ is approximately given by

$$\rho_{\rm n}(T) = \frac{T}{T_{\rm c}} \rho_{\rm n}(T_{\rm c}). \tag{18}$$

II.3. *TAFF(Thermally Activated Flux Flow)*

If the second term of Eq. (14) is smaller than $k_{\rm B}T$, Eq. (1) is written as

$$E \simeq \frac{\pi B a_{\rm f} \nu_0 U_0 J}{J_{\rm c0} k_{\rm B} T} \exp\left(-\frac{U_0}{k_{\rm B}T}\right), \tag{19}$$

and is linear E-J characteristics. This condition is known as TAFF (Thermally Activated Flux Flow). After enough relaxation at high temperature or high magnetic field, TAFF can be observed. Here if J is sufficient small, $U \to U_0$ is achieved and resistivity is given by

$$\rho = \rho_0 \exp\left(-\frac{U_0}{k_{\rm B}T}\right), \tag{20}$$

where ρ_0 is equal to $\pi B a_{\rm f} \nu_0 U_0 / J_{\rm c0} k_{\rm B} T$. From above result, it is found that the resistivity under flux creep does not reach zero due to finite electric field at finite temperature. On the contrary, there are many discussions[7, 8] that if resistivity will be zero at $J \to 0$ which represents real superconducting state ($R = 0$) at finite temperature based on theory of glass-liquid transition of flux lines.

III. FLUX CREEP-FLOW MODEL

In this section, we assume pinning potential, U_0, which is most important parameter in the phenomena of the flux creep. Then, the electric field induced by flux flow is explained. It is shown how to calculate E-J characteristics, critical current density $J_{\rm c}(B)$ and irreversibility field $B_{\rm i}(T)$ based on the flux creep-flow model.

III.1. *Pinning potential, U_0*

Fig. 3 shows the relationship between pinning force density and displacement of flux line. $\widehat{U}_0$ represents pinning potential for unit volume of flux line. When the displacement u is small enough, pinning force density increases linearly, and

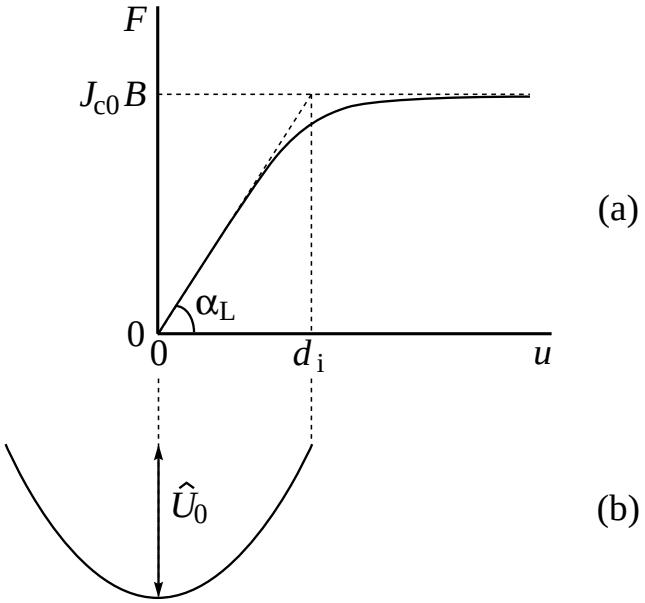

Fig. 3. (a)average pinning force density vs. displacement of flux line. (b) pinning potential for unit volume of flux line, $\widehat{U_0}$.

phenomenon is reversible in this region. On the other hand, it changes to nonlinear and irreversible characteristics, and pinning force density is finally saturated to $J_{c0}B$, when u reaches to interaction distance, d_i. Therefore, $\hat{U}_0$ can be estimated from the present pinning force density-displacement characteristics of reversible region. Here $\hat{U}_0$ is given by

$$\hat{U_0} = \frac{\alpha_L d_i^2}{2}, \tag{21}$$

where α_L is Labusch parameter. Virtual critical current density J_{c0} of flux creep free case is related with α_L and d_i as

$$J_{c0}B = \alpha_L d_i. \tag{22}$$

On the other hand, d_i is given by[4]

$$d_i = \frac{a_f}{\zeta}, \tag{23}$$

where ζ is a constant depended on the kind of pinning center as abovementioned. Then we have pinning potential U_0 of flux bundle as

$$U_0 = \hat{U_0} V, \tag{24}$$

where V is the volume of flux bundle. V is estimated from the size of flux bundle in longitudinal direction, L and transverse direction R given by

$$L = \left(\frac{C_{44}}{\alpha_L}\right)^{1/2}, \tag{25}$$

$$R = \left(\frac{C_{66}}{\alpha_L}\right)^{1/2}, \tag{26}$$

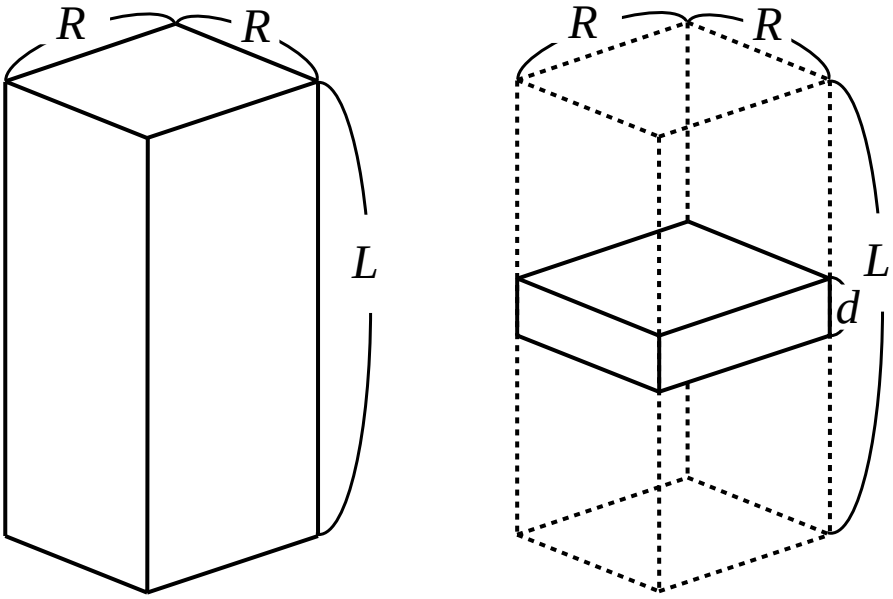

Fig. 4. Volume of flux bundle, V. (a) when longitudinal flux bundle size, L, is smaller than thickness of superconductor, d, $V = LR^2$. (b) when L is larger than d, $V = dR^2$.

as shown in Fig. 4(a). In the above, C_{44} is the tilt modulus of flux lines and given by

$$C_{44} = \frac{B^2}{\mu_0}. \tag{27}$$

On the other hand, C_{66} is the share modulus of flux lines and is largely depended on the condition of flux line lattice. In the case of perfect triangular lattice in three dimensional, C_{66} takes maximum value of C_{66}^0, and it is given by[9]

$$C_{66}^0 = \frac{B_c^2 B}{4\mu_0 B_{c2}} \left(1 - \frac{B}{B_{c2}}\right)^2, \tag{28}$$

and decreases with disorder of flux line lattice, then reaches to zero when flux line lattice is in melt condition.

III.2. *Number of flux lines in the flux bundle, g^2*

It is considered that transverse flux bundle size, R is the order of a_f of several times larger except the case of very week pinning of superconductor. In the case of very strong pinning force, R is smaller than a_f. Although, the size is not smaller than flux line spacing, R is expressed as

$$R = g a_f, \tag{29}$$

where $g^2 (\leq 1)$ is the number of flux lines in the flux bundle. Therefore, g^2 is given by Eqs. (26) and (29)

$$g^2 = \frac{C_{66}}{\zeta J_{c0} B a_f}. \tag{30}$$

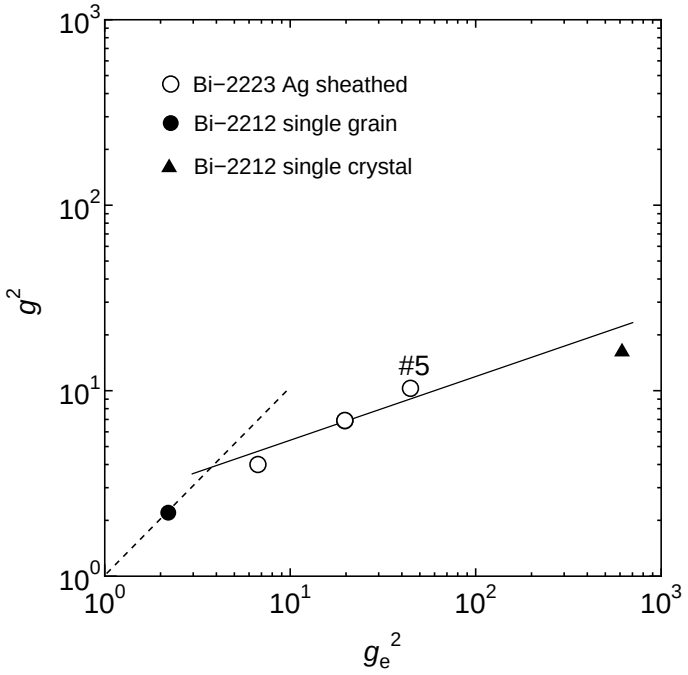

Fig. 5. g^2 obtained from experimental result and g_e^2 predicted by elastic theory[11]. Solid line represents the relation of Eq. (33).

For the case of three dimensional perfect triangle flux line lattice, g^2 takes maximum value, g_e^2, and it is given by[10]

$$g_e^2 = \frac{C_{66}^0}{\zeta J_{c0} B a_f}. \tag{31}$$

As abovementioned, the value of C_{66} is largely depended on the condition of flux line lattice and changes from maximum value of C_{66}^0 to zero, and there is no straightforward method to determine the flux bundle size. Therefore, it is assumed based on "minimization of energy dissipation" that g^2 is determined so as to achieve maximum critical current density under flux creep[11]. According to the theory, g^2 is given as

$$g^2 = g_e^2 \left[\frac{5 k_B T}{2 U_e} \log \left(\frac{B a_f \nu_0}{E_c} \right) \right]^{4/3}, \tag{32}$$

where U_e is the pinning potential at $g = g_e$ and E_c is criteria of electric field, respectively. From the relationship of $U_e \propto g_e$, we have

$$g^2 \propto g_e^{2/3}. \tag{33}$$

In Fig. 5, the relationship between g^2 and g_e^2 is shown. g^2 is obtained from the result of irreversibility field as aforementioned and is quantitatively explained from Eq. (33).

When size of bulk superconductor is larger than L and R, the volume of flux bundle is given by

$$V = LR^2, \tag{34}$$

and the pinning potential is given by

$$U_0 = \frac{0.835 g^2 k_{\rm B} J_{\rm c0}^{1/2}}{\zeta^{3/2} B^{1/4}}. \tag{35}$$

On the other hand, if thickness of superconductor d is smaller than L such as a thin film, V is given by

$$V = dR^2 \tag{36}$$

and U_0 is given by

$$U_0 = \frac{4.23 g^2 k_{\rm B} J_{\rm c0} d}{\zeta B^{1/2}}. \tag{37}$$

III.3. *Irreversibility field*

Before explanation of numerical calculation by the flux creep theory, it is explained that irreversibility is analytically given by U_0 derived in above. First we assumed that the second term in Eq. (15) is neglected. Irreversibility field is given by the field at $J_{\rm c} = 0$ with defined by the electric field criteria $E = E_{\rm c}$. Therefore from Eq. (15) we have,

$$E_{\rm c} = B a_{\rm f} \nu_0 \exp\left(-\frac{U_0}{k_{\rm B} T}\right). \tag{38}$$

If we assume the temperature and magnetic field dependences of $J_{\rm c0}$ as

$$J_{\rm c0} = A\left[1 - \left(\frac{T}{T_{\rm c}}\right)^2\right]^m B^{\gamma-1}\left(1 - \frac{B}{B_{\rm c2}}\right)^\delta \tag{39}$$

where A, m,γ and δ are pinning parameters. Eq. (39) is usually used in conventional metal superconductor and known as scaling law of the critical current density. For the case $d > L$ of larger bulk superconductor, irreversibility field $B_{\rm i}$ is given by

$$B_{\rm i}^{(3-2\gamma)/2} = \left(\frac{K_1}{T}\right)^2\left[1 - \left(\frac{T}{T_{\rm c}}\right)^2\right]^m\left(1 - \frac{B_{\rm i}}{B_{\rm c2}}\right)^\delta. \tag{40}$$

In the above, K_1 is a constant depended on pinning force density as

$$K_1 = \frac{0.835 g^2 A^{1/2}}{\zeta^{3/2}\log(B_{\rm i} a_{\rm f}\nu_0/E_{\rm c})}. \tag{41}$$

On the other hand, for the case $d < L$ such as thin film superconductor, $B_{\rm i}$ is given by

$$B_{\rm i}^{(3-2\gamma)/2} = \frac{K_2}{T}\left[1 - \left(\frac{T}{T_{\rm c}}\right)^2\right]^m\left(1 - \frac{B_{\rm i}}{B_{\rm c2}}\right)^\delta d, \tag{42}$$

where K_2 is given by

$$K_2 = \frac{4.23 g^2 A}{\zeta \log(B_{\rm i} a_{\rm f}\nu_0/E_{\rm c})}. \tag{43}$$

In practical case, $\log(B_{\rm i} a_{\rm f}\nu_0/E_{\rm c})$ can safely be regarded as a constant from 14 to 20, since it is very weakly depended on $B_{\rm i}$.

If temperature is near critical temperature, T_c, B_i is far below upper critical field, H_{c2} and $(1-B_i/B_{c2})^\delta$ in right hand side of Eq. (40) can be regarded as unity. In addition $(K_1/T)^2$ can be approximately put as a constant $(K_1/T_c)^2$. Therefore, the temperature dependence of B_i is given as

$$B_i \propto \left[1-\left(\frac{T}{T_c}\right)^2\right]^{n_i}, \tag{44}$$

where temperature index of irreversibility field, n_i is given by

$$n_i = \frac{2m}{3-2\gamma}. \tag{45}$$

For example, in the case of Y-123, it is known that the parameters are given as $m = 3/2$ and $\gamma = 1/2$, since the dominant pinning center at high temperature is known as Y-211 precipitates. Then we have $n_i = 3/2$ and the temperature dependence of B_i is predicted as $B_i \propto [1-(T/T_c)^2]^{3/2}$. This result is well known as reported by Yeshurun and Malozemoff at very early stage[12].

III.4. *Flux creep-flow model*

For calculation of E-J characteristics, current density is not always smaller than J_{c0}. At $J > J_{c0}$, electric field E_{ff} is induced by flux flow, and is given by

$$\begin{aligned} E_{ff} &= 0; & j \le 1, \\ &= \rho_f(J-J_{c0}); & j > 1 \end{aligned} \tag{46}$$

where ρ_f is given by Eq. (17). On the other hand, electric field by flux creep, E_{cr}, is considered to remain and assumed as[13, 14]

$$\begin{aligned} E_{cr} &= Ba_f\nu_0 \exp\left[-\frac{U(j)}{k_BT}\right]\left[1-\exp\left(-\frac{\pi U_0 j}{k_BT}\right)\right]; \quad j \le 1, \\ &= Ba_f\nu_0\left[1-\exp\left(-\frac{\pi U_0}{k_BT}\right)\right]; \qquad\qquad j > 1. \end{aligned} \tag{47}$$

Then, the total electric field, E, is obtained from E_{cr} and E_{ff} and is approximately given by

$$E = (E_{cr}^2 + E_{ff}^2)^{1/2}. \tag{48}$$

In the above, E is approached to E_{cr} at $j \le 1$ and to E_{ff} at $j \gg 1$.

In usual oxide superconductor, pinning force density is known to be largely distributed. Here only parameter A in Eq. (39) is assumed to have following distribution:

$$f(A) = K\exp\left[-\frac{(\log A - \log A_m)^2}{2\sigma^2}\right], \tag{49}$$

where A_m is most probable value of A, K is normalizing constant and σ^2 is a parameter representing the degree of distribution width of pinning force density. Therefore, total electric field is given by

$$E(J) = \int_0^\infty Ef(A)\mathrm{d}A. \tag{50}$$

III.5. *Summary for numerical calculation*

Here, numerical calculation of E-J characteristics using the flux creep-flow model is summarized. The virtual critical current density in the case of flux creep free case is assumed in Eqs. (39) and (49). Therefore, pinning parameters $A_{\rm m}$, σ, m,γ and δ should be determined. Then, according to the size of superconductor d and L which is given in Eq. (25), pinning potential, U_0, is given by Eqs. (35) or (37).

Electric field by flux creep, $E_{\rm cr}$, can be calculated with U_0 as shown in Eq. (47), where attempt frequency of the flux bundle, ν_0, is given by Eq. (16) and activation energy, U, is given by Eq. (13). On the other hand, electric field by flux flow, $E_{\rm ff}$, can be calculated by Eq. (46) with Eq. (17). Then finally, total electric field, E, is obtained by Eqs. (48) and (50).

IV. RESULTS AND DISCUSSION

In this section, some experimental results in oxide superconductor and other superconductor is compared with theoretical prediction by the flux creep-flow model from references.

IV.1. *E-J characteristics*

E-J characteristics of Bi-2223 silver sheathed tape was investigated by four probe method and relaxation of magnetization by Kodama *et al.*[15]. Figure 6 shows the obtained results of E-J characteristics at 70 K. Four probe method was used for measurement at high electric field region, while the relaxation of magnetization is

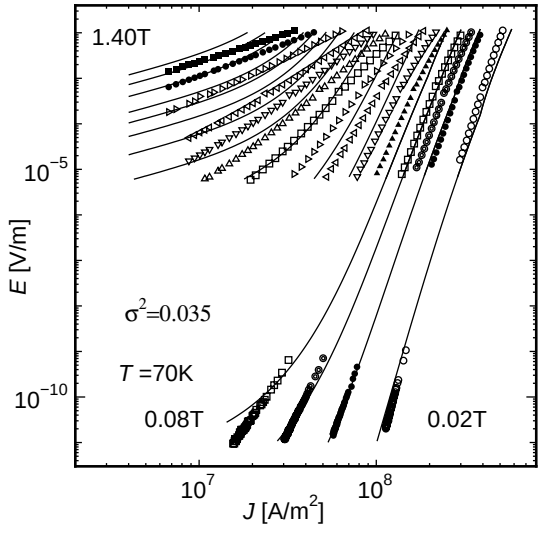

Fig. 6. Comparison of E-J characteristics between experiment (symbol) and theory (lines) at 70 K for Bi-2223 silver sheathed tape. Experimental results are obtained by four probe method at high electric field and the relaxation of magnetization at low electric field.[15]

Table 1. Parameters used for theoretical analysis of magnetic field dependence of J_c of Bi-2223 silver sheathed tape[19]

T_c [K]	$B_{c2\parallel}(0)$ [T]	$\rho_n(T_c)$ [$\mu\Omega$m]	A_m	m	γ	δ	ζ	g^2	σ^2
108.3	50	100	3.0×10^9	4.0	0.87	2.0	2π	1.0	0.18

used at low electric field. It is found that electric field for 9–10 orders of magnitude can be explained by the theoretical prediction of the flux creep-flow model. E-J curve changes from convex to concave according to decreasing electric field at $B = 0.08$ T.

IV.2. *Magnetic field dependence of J_c*

There are several references for comparison of magnetic field dependence of J_c for Bi-2212[16], Y-123[17, 18], Bi-2223[19]. These results of J_c were obtained from numerically calculated E-J characteristics by flux creep-flow model. That is, J_c is determined at criterion of electric field, E_c, such as $E_c = 1 \times 10^{-4}$ V/m for the case of four probe method.

Figure 7 shows the comparison of $J_c(B)$ between experimental and theoretical results of Bi-2223 silver sheathed tape at various temperatures[19]. Table 1 lists the parameters used in the calculation of Fig. 7.

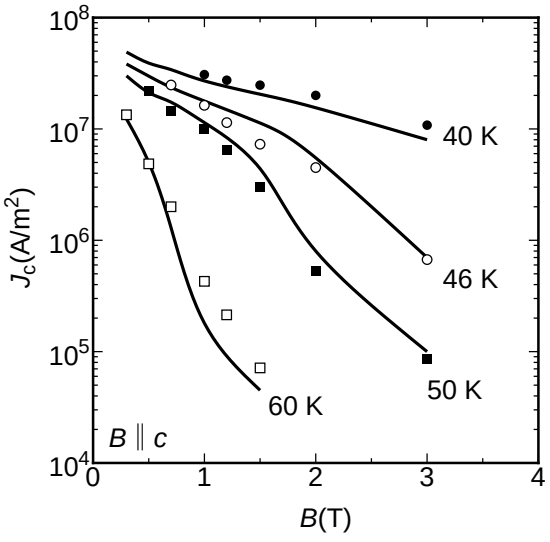

Fig. 7. Comparison of magnetic field dependence of J_c between experiment (symbol) and theory (lines) at various temperatures for Bi-2223 silver sheathed tape.[19]

IV.3. *Irreversibility field*

Theoretical irreversibility field is obtained at the magnetic field where J_c is decreasing to the criteria, ΔJ_c such as $\Delta J_c = 1 \times 10^7$, 1×10^6 A/m^2. An example of comparison of irreversibility field between experimental and theoretical results of Y-123 bulk specimens are shown in Fig. 8.

The irreversibility field is largely depended on the kinds of experimental method with different electric field criterion E_c and ΔJ_c. Figure 9(a) and (b) show dependencies of irreversibility field on electric-field criterion and temperature at $\Delta J_c = 1 \times 10^7$ A/m^2, respectively. It is found that B_i is largely depended on E_c corresponding to

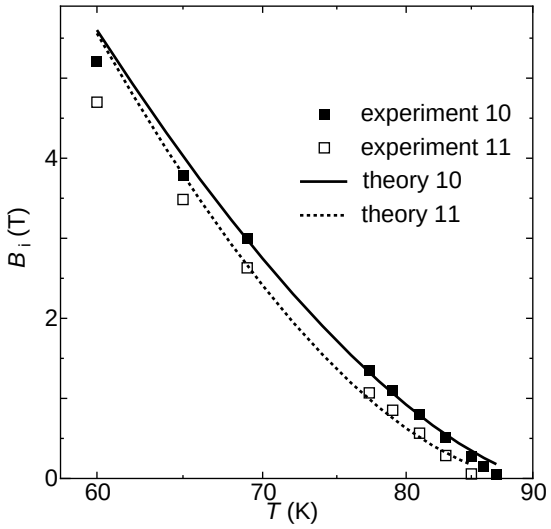

Fig. 8. Comparison of irreversibility field between experiment (symbol) and theory (lines) for two Y-123 bulk specimens.[18]

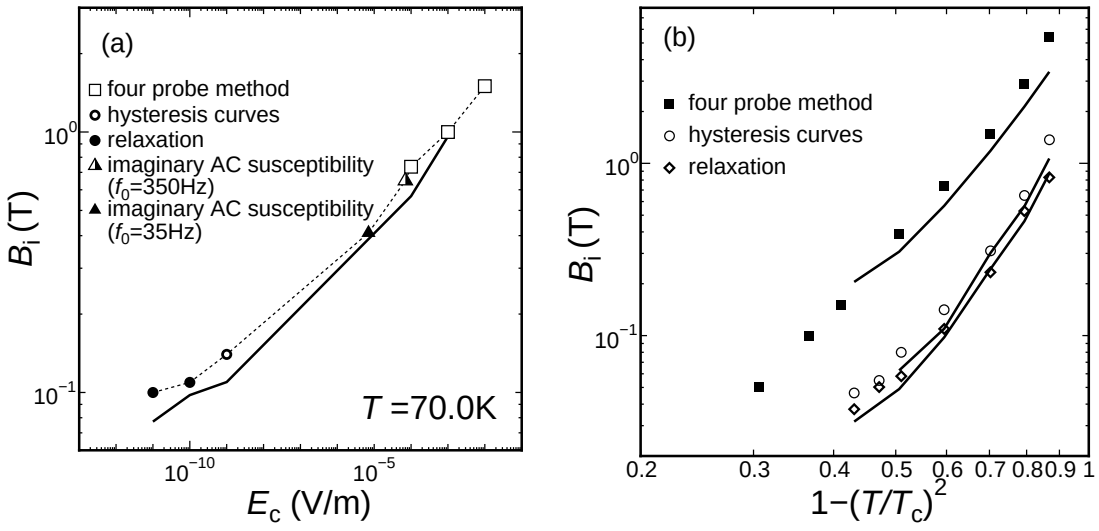

Fig. 9. Dependencies of irreversibility field on (a) electric-field criterion and (b) temperature at $\Delta J_c = 1 \times 10^7$ A/m^2.[20, 21]

Table 2. Fitting parameters according to Eq. (40) for the Bi- Hg-based samples.

sample	T_c [K]	$k = K_1/T_c$	m	γ
Bi-2223 thin film	89	1.2	1.4	0.5
(Bi,Pb)-2223 tape	103	1.0	1.9	0.5
Hg-1223	132	0.92	2.0	0.55
(Hg,Pb)-1223	132	1.2	2.1	0.37

the kinds of experiments. And agreement between experiment and theory is good for wide range of E_c.

IV.4. *Analytical result of irreversibility field*

As mentioned in section III.3., irreversibility field is analytically expressed by Eq. (40). Group of Lüders has investigated the usefulness of Eq. (40) for analysis of irreversibility field in Hg-1223 and Bi-2223 specimens[22, 23]. Table 2 lists T_c and parameters for four investigated specimens. Figures 10 and 11 show fitting results of temperature dependence of irreversibility field for Bi-2223 specimens and Hg-12223 specimens, respectively. It is found that the agreement between theoretical and experimental results is fairly good for wide range of temperature, since factor K_1 is used for temperature dependence of Eq. (40) in this work, which term is usually treated as constant and neglected. Therefore, irreversibility field can be explained by Eq. (40) for the wide temperature range in $0.2 < T/T_c < 1$.

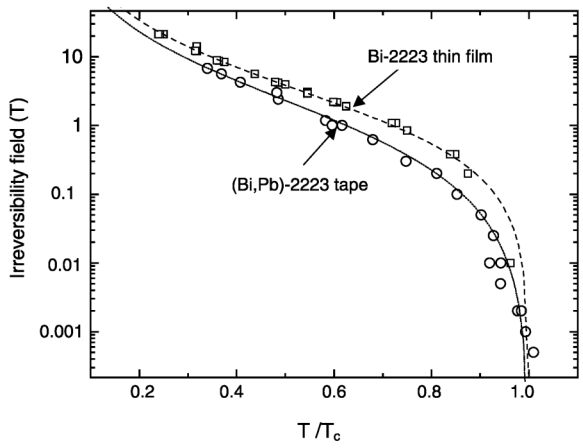

Fig. 10. Temperature dependence of the irreversibility field for the two Bi-based samples. The dotted fit curves correspond to Eq. (40). Fitting parameters are given in Table 2.[22]

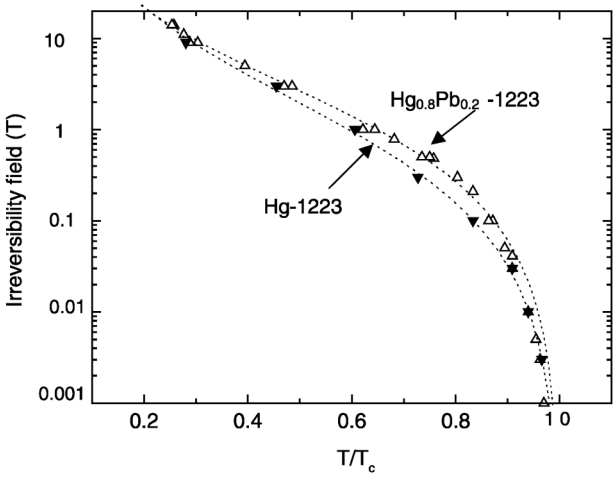

Fig. 11. Temperature dependence of the irreversibility field for the two Hg-based samples. The dotted fit curves correspond to Eq. (40). Fitting parameters are given in Table 2.[22]

IV.5. *Non-oxide superconductor*

The flux creep-flow model is also used for analysis for non-oxide superconductor. In Fig. 12 the theoretical results by flux creep-flow model of J_c of MgB_2 are compared with measured values. Values of the parameters used for the calculation are given in Table 3. J_c was determined with $E_c = 1.0 \times 10^{-9}$ V/m corresponding to the DC magnetization measurement. It is found that the theoretical result agrees well with the experimental result except in high field region at low temperatures. That is, the theoretical result is much higher than the experimental result in this area.

It is important and useful for foreseeing the potential of material for application with using the flux creep-flow model. First the critical current density will be estimated when fine normal precipitates are successfully dispersed in MgB_2. The virtual critical current density in this case is given by [24]

$$J_{c0} = \frac{\pi N_p \xi D^2 \mu_0 H_c^2}{4 a_f B} \left(1 - \frac{B}{\mu_0 H_{c2}}\right)^{\delta}, \tag{51}$$

where N_p and D are density and size of normal particles, respectively, ξ is the coherence length. Here we assume that $D = 0.1$ μm and the volume ratio of normal particles is $N_p D^3 = 0.15$. Equation (51) can be regarded as a most probable value of J_{c0}, and hence we have $m = 3/2$, $\gamma = 1/2$, $\delta = 1$. In addition, $A_m = 4.8 \times 10^9$, $\sigma^2 = 0.03$ and $g^2 = 1.5$ are assumed. Using these parameters the E-J characteristics can be calculated and the critical current density can be defined using the same criterion as in experiment. These results are shown in Fig. 13, in which the present experimental data are also shown for comparison. It is found that a high J_c value can be achieved even at relatively high temperatures.

Table 3. Parameters Used in Numerical Calculation.

A_{m}	σ^2	m	γ	δ	g^2
3.0×10^8	0.03	2.0	0.3	1.0	1.5

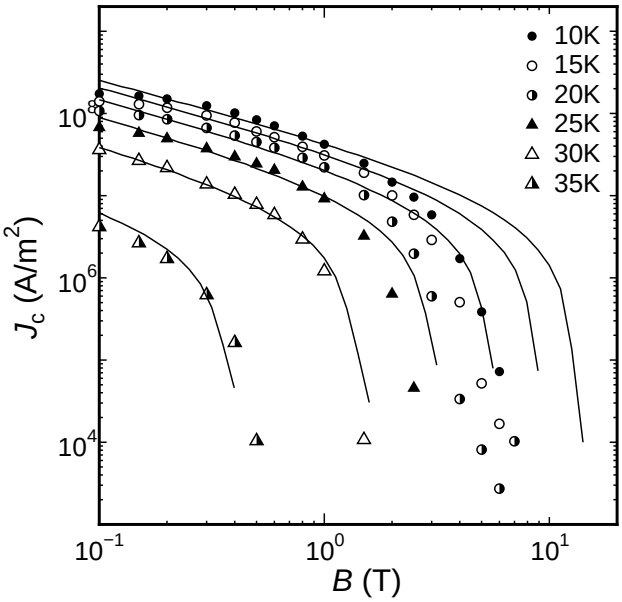

Fig. 12. Theoretically analyzed J_{c} (solid lines) compared with experimental results (symbols) at 10, 15, 20, 25, 30 and 35 K.

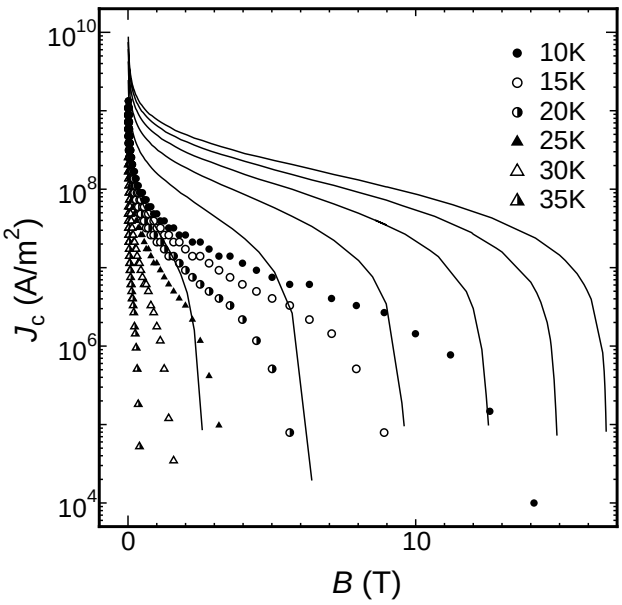

Fig. 13. Calculated J_{c} (lines) assumed effect of normal precipitates compared with previous theoretical results (symbols).

V. CONCLUSION

In this chapter, flux creep phenomenon was explained and some experimental results on E-J characteristics, magnetic field dependence of J_c, temperature dependence of B_i and so on are compared with prediction based on flux creep-flow model. In general, electromagnetic phenomena of superconductor are well described by flux creep-flow model.

REFERENCES

[1] P. W. Anderson and Y. B. Kim: Rev. Mod. Phys. **36** (1964) 39.

[2] D. O. Welch: IEEE Trans. Magn. **27** (1991) 1133.

[3] K. Yamafuji, T. Fujiyoshi, K. Toko and T. Matsushita: Physica C **159** (1989) 743.

[4] A. M. Campbell, H. Kupfer, R. Meier-Hirmer: Proc. Int. Symp. on Flux Pinning and Electromagnetic Properties in Superconductors, Fukuoka (1985) 54.

[5] T. Matsushita: Jpn. J. Appl. Phys. **20** (1981) 1995.

[6] J. Bardeen, M. J. Stephen: Phys. Rev. **140** (1965) A1197.

[7] D. S. Fisher, M. P. A. Fisher and D. A. Huse: Phys. Rev. B **43** (1991) 130.

[8] M. P. A. Fisher: Phys. Rev. Lett. **62** (1989) 1415.

[9] E. H. Brandt: Phys. Rev. B **34** (1986) 6514.

[10] T. Matsushita, T. Fujiyoshi, K. Toko, K. Yamafuji: Appl. Phys. Lett. **56** (1990) 2039.

[11] T. Matsushita: Physica C **217** (1993) 461.

[12] Y. Yeshurun and A. P. Malozemoff: Phys. Rev. Lett. **60** (1988) 2202.

[13] T. Matsushita and N. Ihara: Proc. 7th Int. Workshop on Critical Currents in Superconductors (World Scientific, Singapore, 1994) 169.

[14] T. Matsushita, T. Tohdoh and N. Ihara: Physica C **259** (1996) 321.

[15] T. Kodama, M. Fukuda, S. Nishimura, E. S. Otabe, M. Kiuchi, T. Kiss, T. Matsushita, K. Itoh: Physica C **378–381** (2002) 575.

[16] E. S. Otabe, K. Okamura, H. Wada, M. Kiuchi, T. Yasuda, S. Okayasu, T. Matsushita: IEEE Trans. on Appl. Supercond. **13** (2003) 3083.

[17] T. Matsushita, D. Yoshimi, M. Migita, E. S. Otabe: Supercond. Sci. Technol. **14** (2001) 732.

[18] D. Yoshimi, M. Migita, E. S. Otabe, T. Matsushita: Physica C **378–381** (2002) 788.

[19] M. Kiuchi, K. Noguchi, T. Matsushita, T. Kato, T. Hikata, K. Sato: Physica C **278**, (1997) 62.

[20] T. Matsushita, M. Fukuda, T. Kodama, E. S. Otabe, M. Kiuchi, T. Kiss, T. Akune, N. Sakamoto, K. Itoh: Advances in Cryogenic Engineering, **48** (2002) 1193.

[21] M. Fukuda, T. Kodama, K. Shiraishi, S. Nishimura, E. S. Otabe, M. Kiuchi, T. Kiss, T. Matsushita, K. Itoh: Physica C, **357–360** (2001) 586.

[22] G. Fuchs, K. A. Nenkov, A. Attenberger, K. Lüders, M. Baenitz, C. Ecker, K. Kajikawa, E. V. Antipov, H. R. Khan: Physica C **355** (2001) 299.

[23] P. Shilbe, I. Didshuns, K. Lüders, G. Fuchs, M. Baenitz, K. A. Lokshin, D. A. Pavlov, E. V. Antipov, H. R. Khan: Physca C **372–376** (2002) 1865.

[24] A. M. Campbell, J. E. Evetts: Adv. Phys. 21 (1972) 372.